Presented at the 33rd European PV Solar Energy Conference and Exhibition, 25-29 Sept. 2017, Amsterdam, Netherlands

THE SPEER SOLAR CELL – SIMULATION STUDY OF SHINGLED BIFACIAL PERC-TECHNOLOGY-BASED STRIPE CELLS

Nico Wöhrle, Tobias Fellmeth, Elmar Lohmüller, Puzant Baliozian, Andreas Fell, and Ralf Preu
Fraunhofer Institute for Solar Energy Systems ISE, Heidenhofstraße 2, 79110 Freiburg, Germany
Telephone: +49 761 4588 5964, Fax: +49 761 4588 7621, e-mail: nico.woehrle@ise.fraunhofer.de

ABSTRACT: Increasing the output power density of a photovoltaic module is a reliable way of lowering electricity production costs. Besides increasing the solar cells' conversion efficiency, a further option is lowering electrical and optical cell to module losses. The method of shingling singulated monofacial solar cell stripes is known since Dickson Jr.'s patent in 1956. First, it increases the packing density of active cell area in the module. Second, the active cell area is busbar-less reducing shading losses. Third, due to the reduced area of the solar cell stripes, the generated current per cell is less which results in a reduction of the overall series resistance of the cell interconnection within the module. We call our cell concept for this approach – which is based on the p-type silicon bifacial passivated emitter and rear cell (PERC) concept – "shingled passivated edge, emitter, and rear" – or "SPEER". These cells are then to be interconnected by shingling the p-busbar of the first cell onto the n-busbar of the second cell, constituting the first bifacial shingled module of its kind. Each adjacent shingle covers the busbar with active cell area and minimizes spacing losses in the module. This work covers the optimization of the SPEER concept on cell level with the simulation tool Quokka3. The optimized cell provides the basis for full usage of the cell-to-module gains compared to standard modules. Key issues for optimizing the SPEER cells, which will form the module, concern the characteristics and amount of recombination at their cut edges. This directly affects the question of ideal contour-to-area ratio and thus, the width of the SPEER cells. Using latest experience from bifacial PERC cells and literature values for edge recombination as simulation input, we are able to define a region of interest between 15 mm and 25 mm stripe width for building the first SPEER prototypes. We identify the need for edge treatment, be it an emitter window or edge passivation, as crucial for the success of stripe cells against more conventional cell layouts.
Keywords: bifacial shingle solar cell, PERC, SPEER, stripe cell, Quokka3

1 INTRODUCTION

The first appearance of a shingled solar cell interconnection pattern dates back to 1956 with a US patent filed by Dickson Jr. [1], which is only two years after the first publication of a silicon solar cell by Chapin *et al.* [2]. A number of companies have shown approaches for shingled solar modules. A recent overview can be found in Ref. [3]. Hence, the idea of singulated monofacial solar cells interconnected by a shingling design as such is not a new thing. Early publications of shingling module approaches have been mostly motivated by particular design requirements for specific applications [4, 5]. Later, publications started to make use of the potential for higher module power densities of this technique compared to standard-module cell interconnection, see e.g. Ref. [6]. Consequently, a few large module manufacturers [7, 8] seem to rediscover the potential of monofacial shingling technology to reduce cell-to-module (CTM) losses. The recent International Technology Roadmap for Photovoltaic (ITRPV) projects a world market share of 7% for shingled interconnection technology by 2027 [9].

Another string of technological evolution spreading in the photovoltaic industry is the concept of bifacially illuminated solar cells, which has been extensively covered in a recent article by Kopecek and Libal [10].

As the demand for modules with high power density is large, the opportunity is at hand to combine the bifacial cell technology with the shingle cell module technology. Hereby, the bifacial solar cells profit from additional light coming from the rear side. The busbars on front and rear side for the shingle cells are covered by active area from the adjacent cells, leading to a virtually busbar-free cell string. This combination of features is able to create the highest power density on module-level for silicon PERC technology without concentration of illumination. Another aspect is that this cell/module design does not change the basic ideas of PERC process technology and therefore intrinsically profits from improvements on cell process level, e.g. improved emitter diffusions, surface passivation or bulk carrier lifetimes.

While the conceptual idea of shingled module layouts is to profit from lower CTM-losses compared to standard modules, the development has to start on cell level. Since the standard wafer formats dominate the market, most early approaches for stripe cells will rely on the singulation of a various number of cells out of one 6-inch (pseudo)square wafer. Initially, these stripe cells will face the issue of cleaved (i.e. blank) edges and thus, potentially high edge recombination. Hence, the first focus in the development chain towards shingled modules has to be the singulated solar cell. It has to be designed and processed on cell level in a way that it stays as competitive as possible to full area PERC cells rather than outperforming it by a lot. That is the focus of this work. We call this bifacial stripe solar cell "shingled passivated edge, emitter, and rear cell", or "SPEER". The concept and its true bifacial modelling are both a novelty.

2 APPROACH AND MODEL

The SPEER concept uses (pseudo)square format cells separated into stripes along the busbars. In the module, the cells are interconnected by shingling the p-busbar of the first cell onto the n-busbar of the second cell (see Figure 1). This way the busbars operate only as large pads yielding effectively busbarless strings. Each adjacent shingle covers the busbar with active cell area and minimizes spacing losses in the module. The small stripe size reduces resistive power losses on module level by lowering the total current.

These singulated solar cell stripes have a larger contour-to-area ratio than standard (pseudo)square cells,

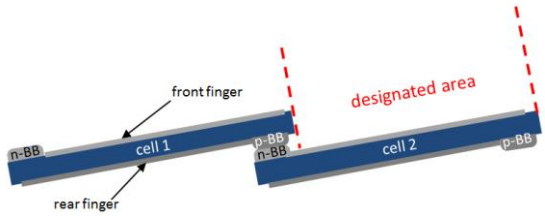

Figure 1: Shingling scheme of two solar cells placing the bottom-busbar of cell 1 onto the top-busbar of cell 2.

which is exemplary shown in Table I for a 2.5 cm- and a 5 cm-wide stripe.

Moreover, (pseudo)square cells undergo passivation processes which also passivate the edges to some extent, while the stripes are singulated after metallization and contact firing leaving the edges initially blank. This poses the question of potential losses by recombination at those edges, which can be divided into three sub-regions for the simulations, sketched in Figure 2:

1. Surfacing bulk region, implicating ideal surface recombination (ideality factor $n = 1$). This can be modeled by using an effective surface recombination velocity between $S_{\mathrm{eff,edge}} = 8$ cm/s for excellent passivation (e.g. reported by Saint-Cast *et al.* [11]) and $S_{\mathrm{eff,edge}} = 5{\cdot}10^6$ cm/s for an unpassivated surface with high defect density (e.g. reported by Glunz and Dicker [12, 13]).
2. Surfacing highly doped emitter region, implicating ideal surface recombination.
3. Surfacing space-charge-region (SCR), implicating non-ideal surface recombination activity (ideality factor $n \approx 2$). Dicker parameterized this recombination for a single recombining edge using the second diode in the two-diode-model naming it $j_{02,\mathrm{edge}}$ [13]. This local recombination current density is determined to be $j_{02,\mathrm{edge}} = 13$ nA/cm, scaling with the contour-to-area ratio. An updated value of $j_{02,\mathrm{edge}} = 19$ nA/cm has been recently published by Fell *et al.* [14], so that $j_{02,\mathrm{edge,tot}} = \mathrm{contour/area}{\cdot}19$ nA/cm². This yields the $j_{02,\mathrm{edge,tot}}$ numbers shown in Table I for exemplary stripe widths.

For the examined cells, Dicker [13] concluded that the recombination of surfacing bulk region and space charge region contribute equally to the total edge recombination while the emitter region surface recombination has negligible influence due to its small extent and is therefore neglected in this study. We will have a closer look into this and distinguish the quality and quantity of recombination influences in the quasi-neutral bulk and the SCR.

The shingling itself (see Figure 1) also has influence on cell optimization. The upper busbar and adjacent area of each cell is covered by active area of the overlying cell. Thus, only the marked designated area is relevant for determination of the short-circuit current density j_{SC}. The model has to consider this fact already on cell simulation level; otherwise the stripe width is optimized under inappropriate assumptions.

Table I: Exemplary calculation for contour-to-area ratio and resulting $j_{02,\mathrm{edge,total}}$ after the formula of Ref. [13] with $j_{02,\mathrm{edge}} = 19$ nA/cm, which shows that a 2.5 cm-wide stripe has almost a fourfold influence on $j_{02,\mathrm{edge,tot}}$ recombination compared to a regular squared cell (for a non-passivated edge).

Stripe/cell size	Contour / area (1/cm)	$j_{02,\mathrm{edge,tot}}$ (nA/cm²)
2.5 x 15.6 cm²	0.93	**17.7**
5.0 x 15.6 cm²	0.53	**10.1**
15.6 x 15.6 cm²	0.26	**4.9**

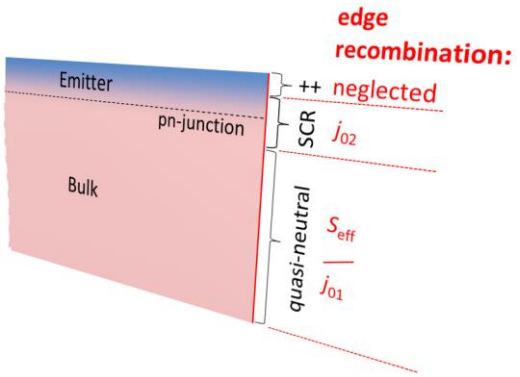

Figure 2: Sketch of the three edge recombination regions used for the simulations with the highly doped area (++), the space-charge-region (SCR), and the quasi-neutral bulk.

A simulation tool which can cover the edge recombination as well as the optical features is the recently developed "Quokka3". Due to a lumped skin approach (an expression originally phrased by Cuevas *et al.* [15]) for non-neutral regions, the mesh fineness can be reduced to a minimum. In consequence, this allows the modeling of much larger domains, in our case a whole cell stripe, resulting in a generalized model without spatial simplifications (opposed to the usual unit cell approach) like potential or series resistance distributions. With the latest addition of a vertical resistance and full injection dependence to the skin parameterization [16], the skins can be described by lumped parameters without error compared to, e.g., explicitly accounting for doping profiles. The cell stripe model is depicted in Figure 3.

The input parameters, summarized in Table II, are taken exemplary from PERC processes available at Fraunhofer ISE to have a representative front side conversion efficiency of 21% under 1000 W/m² AM1.5g illumination and a bifaciality of 75% (see Ref. [17]).

Table II: Simulation input parameters.

Emitter	$j_{0e} = 45$ fA/cm² $j_{0met} = 800$ fA/cm² $R_{sh} = 85$ Ω/sq
Rear side	$j_{0bsf} = 700$ fA/cm² $R_{sh} = 60$ Ω/sq $S_{pass} = 10$ cm/s
Bulk minority carrier lifetime τ_b	500 µs
Finger width	front: 40 µm rear: 150 µm (contact opening: 50 µm)
Busbar width	front: 500 µm rear: 1000 µm
Resistivities	Contact front: $\rho_c = 2$ mΩcm² Ag-finger sheet res.: $R_{sh,f} = 3.15$ mΩ Contact rear: $\rho_c = 5$ mΩcm² Al-finger sheet res.: $R_{sh,f} = 11.7$ mΩ
Optics	random pyramids, 75 nm SiN_x, j_{Ph} (1 sun, no shading) = 41.76 mA/cm²

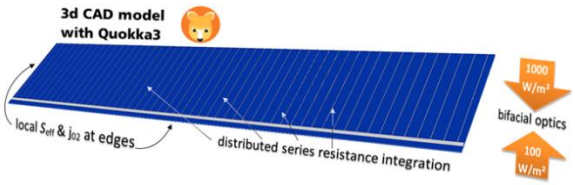

Figure 3: 3D model of a bifacial SPEER solar cell.

Since the publication of the first SPEER simulation results in Ref. [3], the simulation algorithm of Quokka3 has improved: the $j_{02,edge}$ is implemented locally instead of a lumped j_{02}, and the optics model has been updated slightly.

3 EXPERIMENT

We follow the practical process evolution steps of the stripe cell to provide a better understanding of the peculiarities of this concept. The goal of the simulation is to optimize the width of the stripe cell and determine the impact of edge recombination.

The **first simulation** will be the 6-inch pseudo square PERC cell with 205 mm diameter, which serves as reference. The **second simulation** will have a change of layout by virtually slicing the cell right next to the busbar, so that every stripe cell has a "comb-like" metal pattern (Figure 3). The rear grid is 180° rotated, so that the busbar is at the opposite edge than on the front side. Due to the cleaving step, the edges of the stripe cell are potentially highly recombination-active as explained in section 2, thus a negative impact on fill factor *FF* and open-circuit voltage V_{OC} is expected.

In the **third simulation**, the measurement technique is changed to designated area, as explained in section 2 (Figure 1), to optimize the stripe cell in the context of the specific shingle module layout.

The **fourth simulation** is divided in case A and B corresponding to different technical approaches reducing edge recombination:

Case A adds an emitter window, i.e. the diffusion ends 200 µm in front of the edges of the front side, to decouple the recombining edge from the rest of the cell.

Case B, instead, adds edge passivation to reduce the recombination itself. The realization of such an edge passivation technique which is in the best case also suitable for mass production is being examined with high priority in currently ongoing work at Fraunhofer ISE.

As a virtual **side experiment**, located between the third and the fourth simulation, we will separately switch the $j_{01,edge}$- and the $j_{02,edge}$-recombination to work out the separate influence of each recombination region and determine to which degree they add up.

Table III: Applied recombination levels for the cell edges for an unpassivated or a passivated edge.

	$S_{eff,edge}$ (cm/s)	$j_{02,edge}$ (nA/cm)
unpassivated edge	10^6	19
passivated edge	10	0

4 RESULTS

As name convention, we will always use the term output power density p_{out} (mW/cm²) instead of energy conversion efficiency η (%) for measurement data referring to bifacial illumination as it is the less ambiguous unit. The scale is chosen such that with 1000 W/m² monofacial irradiation, the respective numerical value for p_{out} and η are identical.

4.1 Stripe size optimization

The "red star" in Figure 4 represents the **first simulation**, the reference value for the bifacial PERC. It is located at 15.6 mm "stripe width" as this is the equivalent value of the half busbar distance for a five-busbar (5BB) cell and thus has comparable current paths. Under the given illumination of 1000 W/m² front and 100 W/m² rear intensity, p_{out} = 23.4 mW/cm² is obtained.

Cutting this cell intro stripes introduces edge recombination, therefore the **second simulation** features p_{out} = 22.1 mW/cm² for 15.6 mm stripes (orange line). The optimum shifts towards larger stripes of 25 mm width and reaches p_{out} = 22.5 mW/cm². The sliced stripes therefore initially lose 1 mW/cm² towards the full area reference PERC due to *FF* and V_{OC} losses.

Opposed to the reference PERC, the stripe cells will exhibit a shingled layout in the module (Figure 1), and therefore have to be calculated with a designated area excluding the region covered by the overlap of the adjacent cell. This **third simulation** logically increases j_{SC} towards 44 mA/cm² (reminder: 1100 W/m² total irradiance) as the excluded area involves the busbar-shaded region. Moreover it dissolves the dependency of j_{SC} to the stripe width for the same reason, as can be seen in Figure 4b comparing the black and the orange line.

The crucial step to attain the SPEER's competitiveness with the reference is a reduction of edge recombination, performed in the **fourth simulation**.

If this is done by an emitter window of 200 µm inwards from the edge (**Case A**, without edge passivation), V_{OC} increases by roughly 3 mV and *FF* by 1%$_{abs}$ to 2%$_{abs}$ (grey dashed line). The resulting p_{out} = 23.5 mW/cm² for 20 to 25 mm-wide stripes is on par with the reference.

The edge passivated cell (**Case B**, without an emitter window) can exceed the emitter window-cell mainly by a higher *FF*. As a result, the SPEER cell with edge passivation matches the reference cell's *FF* and V_{OC} but exceeds j_{SC} by 1.5 mA/cm² due to larger active cell area (i.e. designated area).

In the end, with high quality edge passivation, the optimal stripe width is located between 15 mm and 20 mm. However the actual preferable stripe size will also depend on handling difficulties in module assembly, which will possibly set a larger lower limit to stripe width.

4.2 Influence of edge recombination types

If the $j_{01,edge}$ and $j_{02,edge}$ recombination are switched separately in the simulation, see Figure 5, one can see the proportional influence of the SCR recombination and base recombination to the total recombination loss of the edges. In Figure 5, both the green dashed line and the black line are identical to the ones in Figure 4.

If $j_{02,edge}$ alone is switched on, the green dashed curve is reduced almost all the way down to the black line. This shows that our SPEER cell is sensitive to the emitter area where it meets the edges. This influence is dominated by the *FF*. On V_{OC}, both $j_{01,edge}$ and $j_{02,edge}$ have similar influence and the changes in j_{SC} are rather small. Additionally it is important to notice that the losses of $j_{01,edge}$ and $j_{02,edge}$ recombination do not add up completely if both are activated.

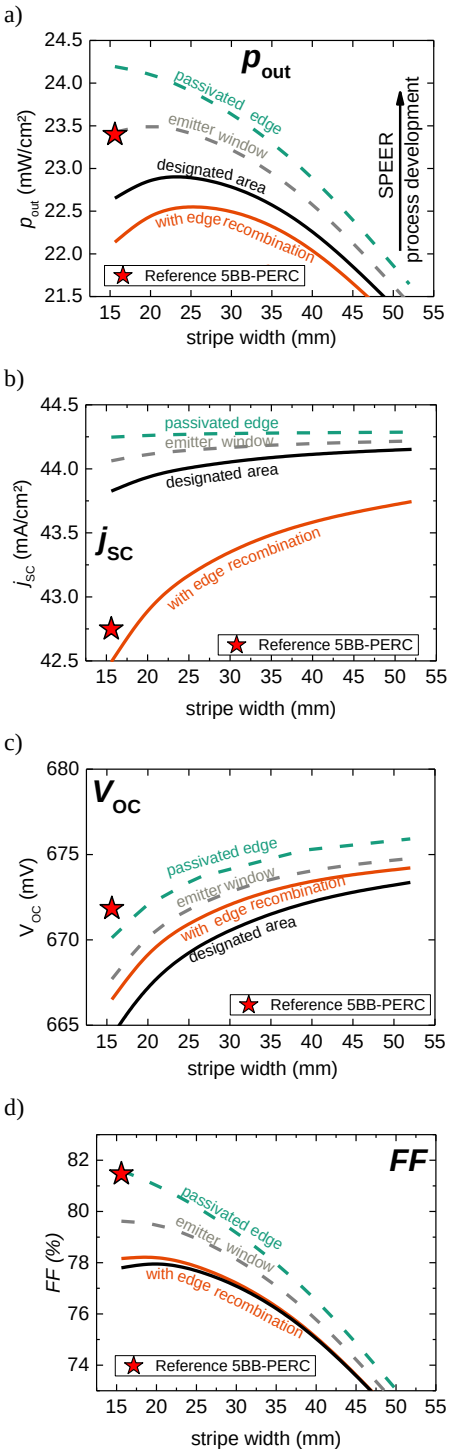

Figure 4: Simulations one to four for the SPEER cell

Current-voltage (*IV*) parameters of the stripe cells at varied cell stripe width for an illumination intensity of 1000 W/m² and 100 W/m² from the front and the rear side, respectively.
First simulation (red star): PERC reference
Second simulation (orange line): $j_{01} + j_{02}$ edge recombination
Third simulation (black line): designated area
Fourth simulation, case A (grey dashes): emitter window
Fourth simulation, case B (green dashes): passivated edge

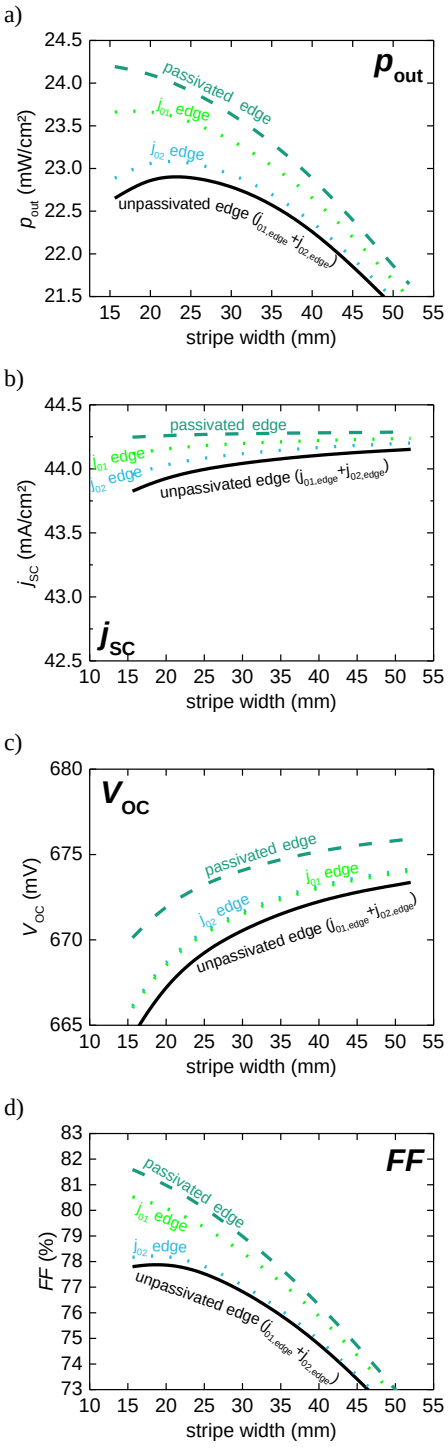

Figure 5: Comparison of influence of edge recombination types

IV parameters of the stripe cells at varied cell stripe width for an illumination intensity of 1000 W/m² and 100 W/m² from the front and the rear side, respectively, with designated area calculation.
Green dashes: passivated edge
Light green dots: j_{01} edge recombination only
Blue dots: j_{02} edge recombination only
Black line: unpassivated edge, $j_{01} + j_{02}$ edge recombination

The explanation is simple: A carrier that has been "consumed" by one recombination type cannot be affected by the second one again. Concerning simulation methodology this means, that both recombination types have to be implemented locally (as Quokka3 does) and not as separate lumped recombination. This would lead to overestimation of the losses.

4 DISCUSSION

The simulation steps 1-4 reflect the process development that has to be made for making the SPEER cell competitive to the full area PERC on cell level.

It is clearly visible that the strip cell layout is initially inferior to a full cell equivalent. On cell level, it accesses its advantages by the projected shingling layout and therefore larger active cell area. This advantage, however, can only be effective if the process-inherent edge recombination losses are minimized. Two suitable approaches are the introduction of an emitter window or an edge passivation.

Reaching this goal ensures the full utilization of the advantages of the shingled module approach which relies on reduced CTM loss towards standard module configurations. Further information about the whole approach of shingled modules can be found in Ref. [3].

5 CONCLUSION

The SPEER solar cell, as cell technology for shingled modules, poses several new challenges in processing, amongst which the most important is the edge recombination. We could show that unpassivated-edge cells have their optimum at 25 mm stripe width, but fall back against the large area PERC reference by 1 mW/cm² or 0.5 mW/cm² (calculated with designated area). The introduction of an emitter window, decoupling the edge recombination from the bulk brings the SPEER on level with the reference. A successful passivation of the edge yields an advantage of 0.7 mW/cm² at 1.1 suns bifacial illumination. The resulting optimal stripe width is located between 15 mm and 20 mm. This value might be influenced by handling considerations in module assembly.

If a suitable edge treatment can be achieved, a shingled module with SPEER cells is put into position to fully access its CTM advantages over a standard module.

6 OUTLOOK

The SPEER solar cell concept is not only a simulation study. The development steps, analogously to the presented simulations, are currently performed at Fraunhofer ISE for PERC as base technology as well as for advanced cell concepts.

ACKNOWLEDGEMENTS

The authors acknowledge the funding of the German Federal Ministry for Economic Affairs and Energy (BMWi) in the frame of the project "PV-BAT400" (contract number 0324145).

REFERENCES

[1] D. C. Dickson, Jr., "Photo-voltaic semiconductor apparatus or the like," US2938938A, USA 2,938,938, May 31, 1960.

[2] D. M. Chapin, C. S. Fuller, and G. L. Pearson, "A new silicon p-n junction photocell for converting solar radiation into electrical power," *J. Appl. Phys.*, vol. 25, no. 5, p. 676, 1954.

[3] N. Wöhrle *et al.*, "Solar cell demand for bifacial and singulated-cell module architectures," *Photovoltaics International*, vol. 36, pp. 48–62, 2017.

[4] J. H. Myer, "Photovoltaic generator," US3369939, US 3,369,939, Feb 20, 1968.

[5] H. Gochermann and J. Soll, "Shingle-type solar cell generator prodn. - allowing formation of curved or domed product," DE3942205C2, Germany 3942205, Feb 1, 1996.

[6] J. Zhao *et al.*, "20000 PERL silicon cells for the "1996 World Solar Challenge" solar car race," *Prog. Photovolt: Res. Appl.*, vol. 5, no. 4, pp. 269–276, 1997.

[7] SunPower Corporation, *SunPower Introduces New Solar Panel: The Performance Series.* [Online] Available: https://us.sunpower.com/blog/2015/11/12/sunpower-introduces-performance-series-solar-panel/. Accessed on: Mar. 21 2017.

[8] B. Yang, P. Nguyen, J. B. Heng, A. Reddy, and Z. Xu, "High Efficiency Solar Panel," US20150090314A1, US 14/563,867, Apr 2, 2015.

[9] ITRPV, "International Technology Roadmap for Photovoltaic: 2016 Results," 2017. [Online] Available: http://www.itrpv.net/Reports/Downloads/.

[10] R. Kopecek and J. Libal, "Quo vadis bifacial PV?," *Photovoltaics International*, vol. 35, 2017.

[11] P. Saint-Cast *et al.*, "High-Efficiency c-Si Solar Cells Passivated With ALD and PECVD Aluminum Oxide," *IEEE Electron Device Lett.*, vol. 31, no. 7, pp. 695–697, 2010.

[12] S. W. Glunz *et al.*, "High-efficiency silicon solar cells for low-illumination applications," in *29th IEEE Photovoltaic Specialists Conference New Orleans*, New Orleans, 2002, pp. 450–453.

[13] J. Dicker, "Analyse und Simulation von hocheffizienten Silizium-Solarzellenstrukturen für industrielle Fertigungstechniken," Dissertation, Fakultät für Physik, Universität Konstanz, Konstanz, 2003.

[14] A. Fell *et al.*, "Modelling edge recombination in silicon solar cells," *IEEE J. Photovoltaics*, submitted, 2017.

[15] A. Cuevas *et al.*, "Skin care for healthy silicon solar cells," in *42nd IEEE Photovoltaic Specialists Conference (PVSC)*, New Orleans, LA, USA, 2015, pp. 1–6.

[16] A. Fell, J. Schön, M. C. Schubert, and S. W. Glunz, "The concept of skins for silicon solar cell modeling," *Solar Energy Materials and Solar Cells*, 2017.

[17] N. Wöhrle *et al.*, "Understanding the Rear-Side Layout of p-Doped Bifacial PERC Solar Cells with Simulation Driven Experiments," *Energy Procedia*, vol. 124C, pp. 225–234, 2017.